Dielectric relaxation study of $Pb_{1-x}La_xMoO_{4+\delta}$ ($x$ = 0–0.3) oxide-ion conductors

# Dielectric relaxation study of Pb$_{1-x}$La$_x$MoO$_{4+\delta}$ ($x$ = 0–0.3) oxide-ion conductors

## G G Zhang, Q F Fang[1], X P Wang and Z G Yi

Key Laboratory of Internal Friction and Defects in Solids, Institute of Solid State Physics,
Chinese Academy of Sciences, Hefei 230031, People's Republic of China

E-mail: qffang@issp.ac.cn

## Abstract

DC conductivity and dielectric relaxation measurements are exploited to study
the influence of La substitution on the dielectric properties and oxygen-ion
transportation in PbMoO$_4$ samples. The DC conductivity of La-doped samples
is about $10^{-3}$ S cm$^{-1}$ around 1073 K. A dielectric loss peak with activation
energy of 0.6–0.8 eV is observed in the temperature spectrum as well as in
the frequency spectrum for all La-doped PbMoO$_4$ samples. With increasing
La doping content, this peak becomes higher and shifts to higher temperature
or lower frequency, and the activation energy becomes larger. It is suggested
that this dielectric loss peak is associated with the short-distance diffusion of
oxygen ions (or oxygen vacancies) between the 16f and 8e sites of the scheelite
structure type with $I4_1/a$ symmetry.

## 1. Introduction

Oxygen-ion conducting materials are attracting more and more attention owing to their
applications in the fields of solid oxide fuel cells (SOFC), oxygen sensors, oxygen pumps and
catalysts for selective oxidation. Among these materials, yttria-stabilized zirconia (YSZ) [1–
4], doped ceria [5], doped lanthanum gallate [6] and lanthanum molybdate [7–12] are
the most widely investigated because of their high oxygen-ion conductivity. From the
structural viewpoint, these materials commonly possess oxygen vacancies. Recently, doped
scheelite-type PbWO$_4$ oxides have been reported as oxide-ion conductors [13, 14]. In the
Pb$_{1-x}$La$_x$WO$_{4+\delta}$ ($\delta \approx x/2$) system, for example, the extra oxygen ions introduced by La
doping seem to be rather localized around $z = 0.3$ of the 8e position (00$z$) of the scheelite
structure with $I4_1/a$ symmetry. These positions are apparently not fully occupied and will act
as possible paths for oxygen-ion migration.

---

[1] Author to whom any correspondence should be addressed.

Wulfenite $PbMoO_4$ crystals also possess a scheelite structure with a tetragonal space group $I4_1/a$, and would behave as a good oxide-ion conductor if doped with trivalent cations such as lanthanum. In $PbMoO_4$, the $Pb^{2+}$ ion has a lone pair ($6s^2$ electrons), which usually occupies a volume similar to that of the oxygen anion. According to the LPS concept in the design of oxide-ion conductors [8], substituting $Pb^{2+}$ and its lone pair with $La^{3+}$ is likely to create a vacancy or vacancy/anion sublattice in place of the original lone-pair lattice, namely the partial occupation of oxygen ions in the 8e sites as in the case of La-doped $PbWO_4$. In this paper, we have prepared pure and La-doped $PbMoO_4$ samples by adding 5 wt% extra PbO in the raw powders in order to diminish the lead vacancies as much as possible. The dielectric loss and dynamic dielectric constant measurements are exploited to study the effect of La doping and the behaviour of oxygen vacancies.

## 2. Experimental details

Ceramic samples of $Pb_{1-x}La_xMoO_{4+\delta}$ ($x = 0, 0.1, 0.2, 0.3$) are prepared by conventional solid-state reaction from a stoichiometric mixture of $La_2O_3$, $MoO_3$ and PbO powders. Empirically, about 5 wt% extra PbO powders are added to compensate for the evaporation of PbO in the sintering process. The well-mixed powders are calcined in an alumina crucible at 923 K for 15 h in air, and then finely ground and pressed into discs (about 20 mm in diameter and 2 mm in thickness). These disc samples are finally sintered at 1123 K for 10 h in air. Silver paste is applied onto both sides of the sample and heated at 1073 K for 30 min as the electrodes. The DC conductivity is obtained by supplying a constant direct current to the sample and measuring the voltage difference between the two ends of the sample in the temperature range from 523 to 973 K. Although this two-probe method for conductivity measurement is less accurate than the four-probe method owing to the existence of a counter voltage, it can give a good approximation of the conductivity of the sample in the case of low conductivity. The x-ray diffraction (XRD) data are collected at room temperature with Cu K$\alpha$ radiation. The dielectric relaxation measurements are carried out using a Hioki 3531 Z Hitester, which covers the frequency range from 50 Hz to 5 MHz. The frequency dependence of the dielectric loss (tan $\delta$) and the dynamic dielectric constant ($\varepsilon'$) are measured every 25 K from 423 to 523 K with the frequency scanning from 50 Hz to 5 MHz. The temperature dependence of tan $\delta$ and $\varepsilon'$ are measured at 1, 5, 10, 50 and 100 kHz with ascending temperature.

## 3. Experimental results

Figure 1 shows the XRD of the $Pb_{1-x}La_xMoO_{4+\delta}$ ($x = 0, 0.1, 0.2, 0.3$) samples. These patterns can be well indexed into a tetragonal structure of space group $I4_1/a$ with lattice constants of about $a = 5.4$ Å and $c = 12.1$ Å, except for some small diffraction peaks around $31.25°$, $32.3°$, $45.4°$ and $54.5°$, which increase in relative intensity with increasing La doping and can be ascribed to the phase of cubic $La_2Mo_2O_9$ of space group $P2_13$. These three peaks, together with the possible component superimposed on the main peaks of space group $I4_1/a$, indicate that a small amount of $La_2Mo_2O_9$ phase appears. The lattice constants of $Pb_{1-x}La_xMoO_{4+\delta}$ phase are deduced from the XRD patterns by the line-profile refinement method described by Rietveld [15], and listed in table 1. Both $a$ and $c$ decrease slightly with increasing La doping due to the smaller ionic radius of La ions.

Variations of the DC conductivity (on a logarithmic scale) with the reciprocal of temperature are shown in figure 2 for the three $Pb_{1-x}La_xMoO_{4+\delta}$ ($x = 0, 0.1, 0.2, 0.3$) samples. For the pure $PbMoO_4$ sample the DC conductivity is low. For the 10% La-doped
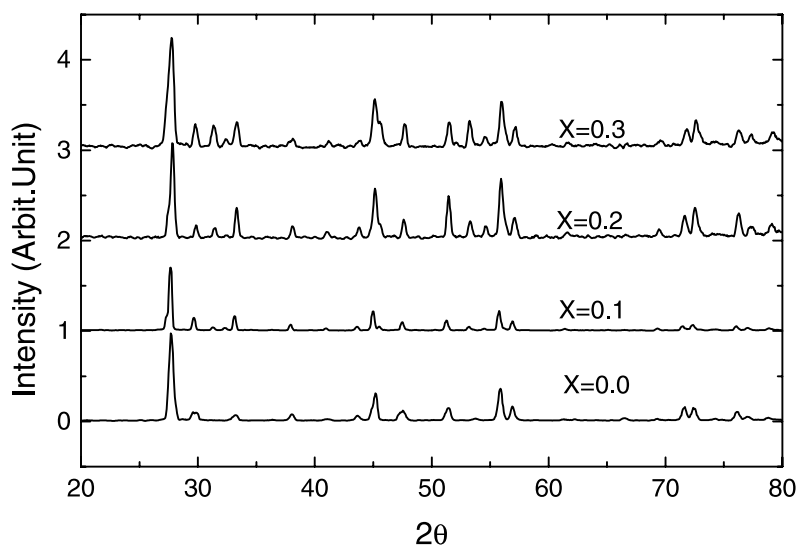
**Figure 1.** X-ray diffraction pattern of Pb$_{1-x}$La$_x$MoO$_{4+\delta}$ ($x = 0$, 0.1, 0.2, and 0.3) collected at room temperature.

**Table 1.** Pre-exponential factor ($\tau_0$) and activation energy ($E$) of the dielectric relaxation peak, and the lattice constants ($a$ and $c$) for three Pb$_{1-x}$La$_x$MoO$_{4+\delta}$ samples ($x = 0.1, 0.2, 0.3$).

| La doping content | $x = 0.1$ | $x = 0.2$ | $x = 0.3$ |
|---|---|---|---|
| $\tau_0$ ($10^{-13}$ s) | 9 | 2 | 15 |
| $E$ (eV) | 0.57 | 0.71 | 0.77 |
| $a/c$ (Å) | 5.430/12.106 | 5.428/12.094 | 5.406/12.049 |

sample, the logarithm of DC conductivity increases linearly with the decrease of the reciprocal of temperature and is larger than that for the pure PbMoO$_4$ sample. The conductivity of the 20% doped sample is larger than that of the 10% doped one in the whole measured temperature range, and reaches about 0.001 S cm$^{-1}$ if it is extrapolated to 1073 K, which is about several tens of times lower than that of the Pb$_{0.8}$La$_{0.2}$WO$_{4.1}$ sample deduced from the AC impedance measurement at 10 kHz [16]. In this sample, the DC conductivity changes abnormally around 715 K, indicating a slight structural change. For the 30% doped sample, the conductivity is similar to that of the 20% doped sample, but the temperature range where the DC conductivity changes abnormally shifts to around 800 K. At temperatures greater than 800 K and less than 640 K, the DC conductivity of the 30% doped sample becomes smaller than that of the 20% doped sample. The structural change may be an order–disorder phase transition as observed in La$_2$Mo$_2$O$_9$ [7–12].

Figure 3 shows the temperature dependence of dielectric loss (tan $\delta$) and the dynamic dielectric constant ($\varepsilon'$) for the Pb$_{1-x}$La$_x$MoO$_{4+\delta}$ samples ($x = 0, 0.1, 0.2, 0.3$) at 5 kHz. Figure 4 shows the frequency dependences of tan $\delta$ and $\varepsilon'$ for the three samples at 523 K. A prominent dielectric loss peak appears in the temperature spectra (figure 3) as well as in the frequency spectra (figure 4) for the La-doped samples, accompanied by a dramatic change in the dielectric constant, while for the pure PbMoO$_4$ sample both the dielectric loss and the dielectric constant change smoothly and no peak appears. As the La doping concentration increases, the relaxation peak becomes higher and shifts to a higher temperature (in the temperature
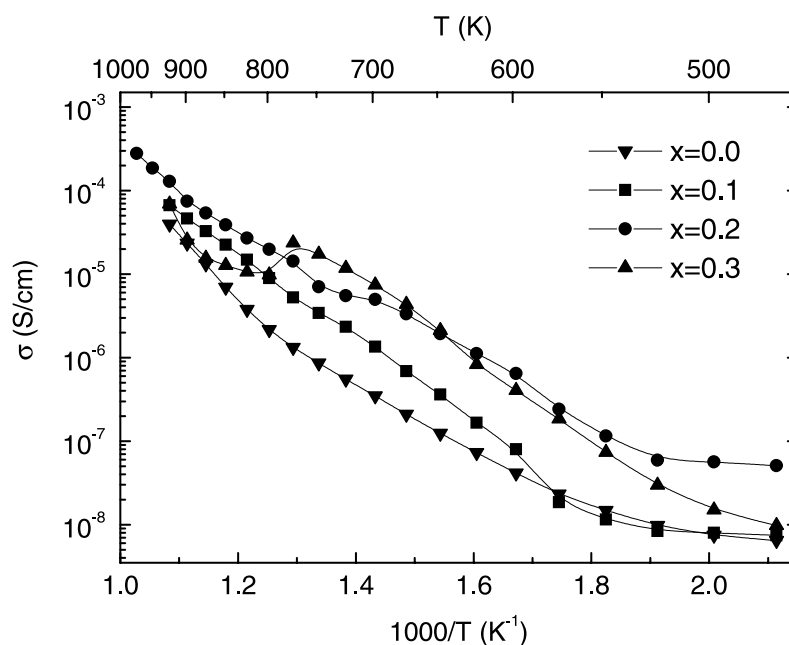
**Figure 2.** Variation of the DC conductivity ($\sigma$) with the reciprocal of temperature for three Pb$_{1-x}$La$_x$MoO$_{4+\delta}$ samples ($x = 0.1$, 0.2 and 0.3).

spectra) or to a lower frequency (in the frequency spectra). In figure 3, for the 30% La-doped sample, a stepwise change appears at 800 K. If we measure the temperature spectrum at different frequencies, this stepwise change locates at the same temperature. This phenomenon is a manifestation of the phase transition as observed at the same temperature in the DC conductivity measurement.

Generally, background dielectric loss on the low-frequency side in the frequency spectra or the high-temperature side in the temperature spectra is attributed to the DC conductivity contribution and can be expressed as $\tan \delta = \frac{\sigma}{\omega \cdot \varepsilon}$, where $\sigma = \sigma_0 \exp(-E_{cond}/kT)$ is the DC conductivity, $\omega = 2\pi f$ is the angular frequency and $\varepsilon$ is the permittivity. Therefore, the background $\tan \delta$ will vary exponentially in the plot of $\tan \delta$ versus $1/T$ or $\tan \delta$ versus $\log(\omega)$, and its magnitude is proportional to the DC conductivity. However, the pure PbMoO$_4$ sample with lower DC conductivity has a comparable or even larger background $\tan \delta$ than the doped samples, as shown in figures 3 and 4. This can be understood from the fact that the permittivity (proportional to $\varepsilon'$ in figures 3 and 4) of the pure PbMoO$_4$ sample is about several tens of times lower than that of the doped samples in the background region, which will enlarge the background $\tan \delta$. The exponential variation behaviour of background $\tan \delta$ at high temperatures in figure 3 is apparent and the relative magnitude of background $\tan \delta$ of the three doped samples (in the descending order 20, 30, 10% doped samples) is in accordance with their DC conductivity measurement results below 640 K as shown in figure 2. In figure 4, however, the exponential variation behaviour of background $\tan \delta$ at low frequencies is not apparent in the measurement frequency window, which can be understood from the low DC conductivity at such a low measurement temperature (523 K).

For each sample, the dielectric loss peak shifts to higher temperatures with increasing frequencies (in temperature spectra) and/or to higher frequencies with increasing temperature
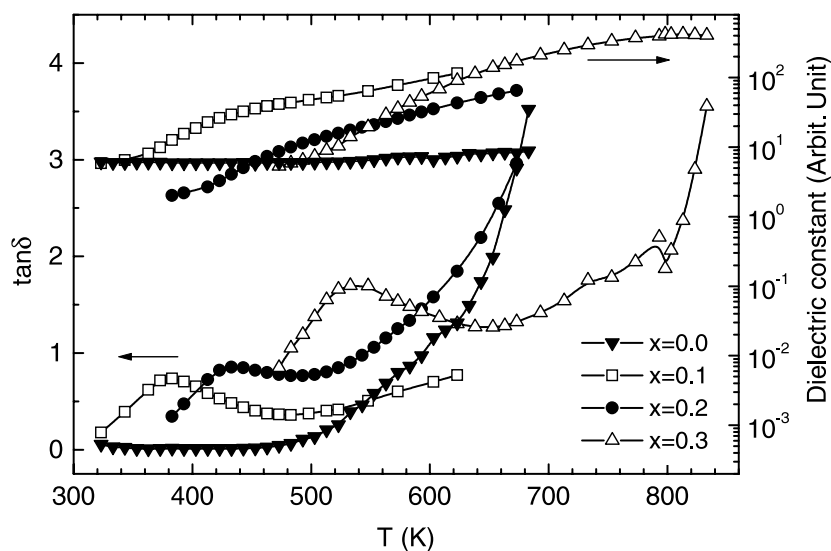
**Figure 3.** The temperature dependence of dielectric loss and dynamic dielectric constant of Pb$_{1-x}$La$_x$MoO$_{4+\delta}$ ($x = 0$, 0.1, 0.2 and 0.3) samples at 5 kHz.
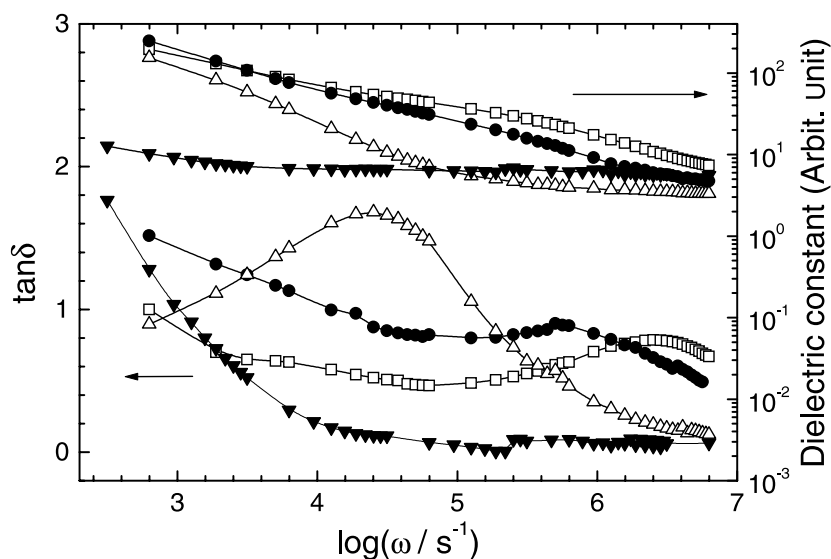


**Figure 4.** The frequency dependence of dielectric loss and dynamic dielectric constant of Pb$_{1-x}$La$_x$MoO$_{4+\delta}$ ($x = 0$, 0.1, 0.2 and 0.3) samples at 523 K (▼: $x = 0$, □: $x = 0.1$, ●: $x = 0.2$, △: $x = 0.3$).

(in frequency spectra), indicating the relaxation nature of this peak. Because for a relaxation peak $\omega\tau = 1$ at the peak position, one can get the value of relaxation time $\tau$ at the peak position, where $\omega = 2\pi f$ is the angular frequency and $f$ is the measurement frequency. The values of $\tau$ at the peak position are calculated as the reciprocal of the measurement angular frequency in the temperature spectra, and as the reciprocal of the peak angular frequency in the frequency spectra. According to the Arrhenius law, $\tau = \tau_0 \exp(E/kT)$, where $\tau_0$ is the
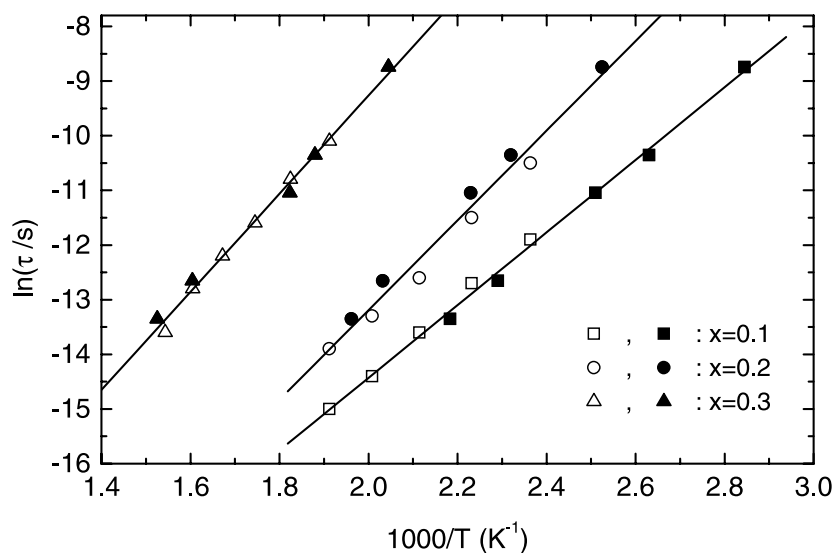
**Figure 5.** Plots of the relaxation time ($\tau$) versus reciprocal of peak temperature for three $Pb_{1-x}La_xMoO_{4+\delta}$ samples ($x = 0.1$, 0.2, and 0.3). The solid symbols represent the data obtained from the temperature spectrum and the open symbols are data obtained from the frequency spectrum. The solid lines are linear least-square fittings.

pre-exponential factor, $E$ is the activation energy of the relaxation process, $T$ is the absolute temperature and $k$ is Boltzmann constant, the activation energy can be deduced from the shift of peak position with frequency in the temperature spectra and/or with temperature in the frequency spectra. The relation between $\ln(\tau)$ and the reciprocal of the peak temperature (or measurement temperature in the case of frequency spectra) is plotted in figure 5, where the lines are linear fittings. The activation energies and the $\tau_0$s of the three samples deduced from the slopes and the intercept of the lines, which are in the ranges of 0.6–0.8 eV and $\sim 10^{-13}$ s, respectively, are listed in table 1. The activation energy increases with increasing La doping content.

## 4. Discussion

In the $Pb_{1-x}La_xMoO_{4+\delta}$ samples there are two lattice sites for oxygen accommodation, i.e. 16f and 8e sites of the scheelite-type structure with $I41/a$ symmetry, as shown in figure 6. The 8e sites are partially occupied and the occupation rate is equal to $x/4$. In the pure $PbMoO_4$ samples half of the 8e sites are regularly occupied by the lone-pair electrons of $Pb^{+2}$ ions, which will prevent the oxygen ions diffusing through the 8e sites. This is the reason why in the pure $PbMoO_4$ samples the ionic conductivity is low and the relaxation peak does not appear. In the case of La doping, two La ions substituting two Pb ions will free two 8e sites occupied previously by the lone-pair electrons, one of which will be occupied by an oxygen ion introduced to compensate the increase of cationic valence. These free 8e sites will increase with La doping content and provide an easier path for oxygen-ion diffusion [14], and therefore the ionic conductivity of the oxide increases and a relaxation peak appears.

Concerning the mechanism of the dielectric relaxation peak, we suggest that the short-distance diffusion of oxygen ions (or vacancies) between 8e and 16f sites would be responsible. The theory of point defect relaxation [17] predicts that the relaxation strength has a linear
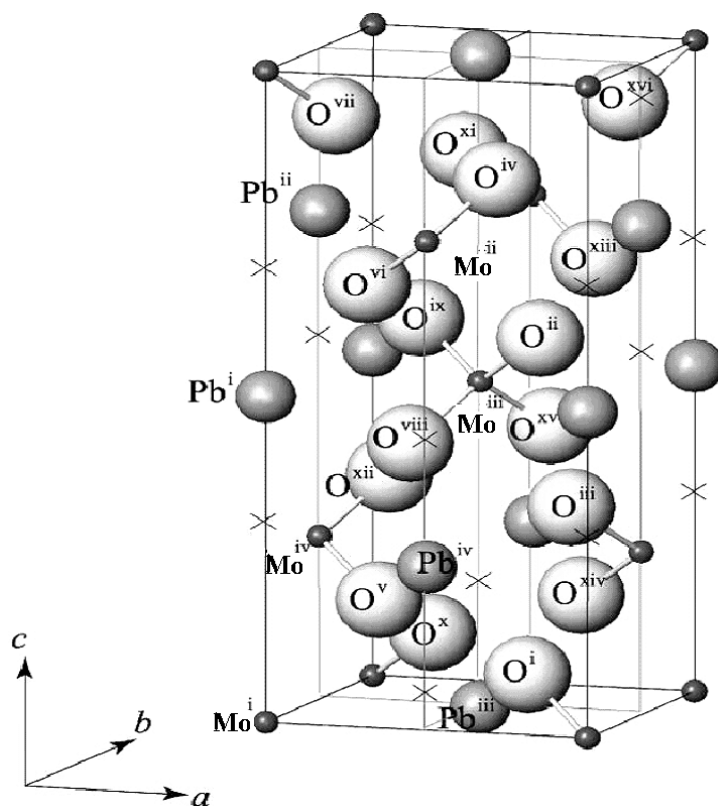
**Figure 6.** Schematic view of a unit cell of scheelite-type structured $PbMoO_4$. Pb, Mo and O atoms are represented by medium, small and large spheres. The 8e sites $(00z)$ of $I41/a$ symmetry with the equivalent position are depicted by the thin cross marks. Four sites for Mo ($Mo^I$–$Mo^{IV}$), four sites for Pb (or La) ($Pb^I$–$Pb^{IV}$) and 16 sites for O ($O^I$–$O^{XVI}$) atoms are numbered.

dependence on the defect concentration and the square of the dipole shape factor based on the concept that each point defect (e.g. oxygen vacancy) creates an elastic or electric dipole. Considering the high oxygen vacancy concentration at 16f and 8e sites, the possibility of migration between 16f and 8e is large enough to produce a dielectric relaxation peak with strength of the order of magnitude of 1. Because the site symmetry of these two sites is different and lower than that of the crystalline lattice, the back and forth jumps of oxygen vacancies (or ions) between these two sites would give rise to a relaxation peak under appropriate conditions.

Based on the structure shown in figure 6, a possible long-distance migration path for oxygen ions through vacancies was suggested in [14], for example $O^V \leftrightarrow O^E \leftrightarrow O^{XIV} \leftrightarrow O^E \leftrightarrow O^V$, where $O^E$ denotes the oxygen ions at 8e sites. That is to say, a long-distance migration path consists of a series of short-distance jumps of oxygen ions (or vacancies) between 8e and 16f sites. The experimental fact that the peak height increases with La doping content can be understood under this mechanism because the relaxation strength is proportional to the concentration of the relaxation species (here the oxygen vacancies in 8e sites). The increase of the activation energy of the relaxation peak with La doping can be explained by the decrease of the lattice constant with La doping, as the smaller free volume in the unit cell will hinder the oxygen-ion diffusion.

A similar dielectric relaxation peak is observed in $PbWO_4$ single crystals slightly doped by lanthanum, which was suggested to be associated with the short-distance diffusion of

dipole complexes of lanthanum ions and lead vacancies [18], instead of oxygen vacancies. This suggestion is not appropriate in our case because the Pb deficiency produced by the La doping is reported only in samples of $Pb_{1-x}La_{2x/3}WO_y$ but not in $Pb_{1-x}La_xWO_y$ [19]. The co-appearance of the oxide ionic conduction and the relaxation peak illustrate from another side that the mechanism of this relaxation peak corresponds to the short-distance diffusion process of oxygen ions.

## 5. Conclusion

The La-doped $PbMoO_4$ samples exhibit a dielectric relaxation peak in the temperature spectra as well as in the frequency spectra. This peak has activation energies of 0.6–0.8 eV depending on the La-doping content and can be explained by the short-distance diffusion of the oxygen ions (or vacancies) between the 8e sites and 16f sites. The DC conductivity of $PbMoO_4$ samples doped with 10–30% La has a value of about $10^{-3}$ S cm$^{-1}$ around 1073 K.

## Acknowledgment

## References

 [1] Pimenov A *et al* 1998 *Solid State Ion.* **109** 111
 [2] Weller M and Schubert H 1986 *J. Am. Ceram. Soc.* **69** 573
 [3] Wang D Y and Nowick A S 1983 *J. Phys. Chem. Solids* **44** 639
 [4] Sammells A F *et al* 1992 *Solid State Ion.* **52** 111
 [5] Hibino T *et al* 2000 *Science* **288** 2031
 [6] Huang K, Tichy R S and Goodenough J B 1998 *J. Am. Ceram. Soc.* **81** 2565
 [7] Lacorre P *et al* 2000 *Nature* **404** 856
 [8] Lacorre P 2000 *Solid State Sci.* **2** 755
 [9] Goutenoire F, Isnard O and Lacorre P 2000 *Chem. Mater.* **12** 2575
[10] Wang X P and Fang Q F 2001 *J. Phys.: Condens. Matter* **13** 1641
[11] Wang X P and Fang Q F 2002 *Solid State Ion.* **146** 185
[12] Wang X P and Fang Q F 2002 *Phys. Rev.* B **65** 064304
[13] Esaka T 2000 *Solid State Ion.* **136/137** 1
[14] Takai S *et al* 2002 *Solid State Ion.* **148** 123
[15] Rietveld H M 1969 *J. Appl. Crystallogr.* **2** 65
[16] Esaka T, Mina-ai T and Iwahara H 1992 *Solid State Ion.* **57** 319
[17] Nowick A S and Berry B S 1972 *Anelastic Relaxation in Crystalline Solids* (New York: Academic)
[18] Han B G *et al* 1998 *J. Appl. Phys.* **84** 2831
[19] Takai S *et al* 2000 *Solid State Ion.* **138** 161